Lightning Hole and Lightning Jump Relationships in the PERILS Campaign

ALAINA A. ADDERLEY[1] AND VANNA C. CHMIELEWSKI[2] AND SARAH M. STOUGH[3*]

[1]*National Weather Center Research Experiences for Undergraduates Program*
Norman, Oklahoma.

[2]*NOAA/OAR/National Severe Storms Laboratory*
Norman, Oklahoma

[3]*Cooperative Institute for Severe and High – Impact Weather Research and Operations, University of Oklahoma*
Norman, Oklahoma

ABSTRACT

Lightning holes and lightning flash rate patterns, including jumps and dives, are known to be related to a storm's updraft intensity. However, relationships between these spatial and temporal lightning patterns are not well defined despite their common dependency on the updraft. Understanding these patterns could help with early warnings and forecast confidence. This paper analyzes a storm observed in Mississippi and Alabama during the Propagation, Evolution, and Rotation in Linear Storms (PERiLS) field campaign using Lightning Mapping Array (LMA) and radar data. This storm initiated ahead of and eventually merged with a quasi-linear convective system (QLCS). This evolution is especially interesting as lightning hole presence in QLCSs and mixed-mode storms has not been well documented in prior publications. The presentation of the lightning hole changed, with respect to altitude, as the merge occurred.. In this case, the lightning hole initiated in the mid-levels of the storm and expanded vertically. During these vertical expansions and contractions of the lightning hole, the flash rates varied alternatively between increasing and decreasing patterns. When the flash rates were at their highest, after the merge into the QLCS, the lightning hole was present throughout the deepest layers of the storm.

1. Introduction

Lightning is a continuous dataset that can be used to complement radar data and cover times of low temporal resolution. Together, these can be used to aid in warning lead times and increase forecaster confidence in their decisions. Lightning can be used as an early indicator of storm intensification due to the behavior of the updraft. The primary mechanism for electrification is the charge separation between ice crystals and graupel, known as non-inductive collisional charging (Takahashi et al. 1984). Non-inductive collisional charging is affected by particle size, velocity, and distributions in favorable conditions for electrification, all of which are affected by the strength of the updraft (Schultz et al. 2009; MacGorman et al. 2005). A resulting change in flash rates can be indicative of storm intensity and hint at future behavior.

A lightning jump or a lightning dive is a storm-scale flash rate pattern characterized by a rapid increase or decrease, respectively, in flash rates (Williams et al. 1999; Schultz et al. 2009; Vacek et al. 2017). In a Florida study, isolated storms were found to have a lightning jump 5-20 minutes before storm intensification (Williams et al. 1999). An average of 23 minutes lead time was discovered in a study in northern Alabama and Tennessee looking at a variety of storm modes such as mesoscale convective systems, supercells, and tropical remnant tornadic rainbands (Schultz et al. 2009). Lightning jumps and dives could also be a potential indicator of tornadogenesis. Studies have found that a lightning jump can occur prior to tornadogenesis with the intensification of the updraft, and a lightning dive can occur after the tornado initiates (Steiger et al. 2007; Vacek et al. 2017; Darden et al. 2010; Stough et al. 2017). However, lightning jumps do not always precede tornadogenesis; in many cases, they precede other phenomena such as hail or severe winds (Williams et al. 1999; Vacek et al. 2017) or can occur without observations of subsequent severe weather. Some tornadic cells produce little to no lightning for the duration of their life (Schultz et al. 2009); limiting the usefulness of lightning trends. With the large variety of storm modes, there is much to be researched in this area.

Lightning holes are another lightning pattern, though different from lightning jumps, as they are a spatial pattern, not a temporal one. Lightning holes are defined as an area of little to no lightning activity centered around the updraft or the Bounded Weak Echo Region (BWER).

*Corresponding author address: Alaina Adderley, Plymouth State University, 17 High St, Plymouth, NH 03264
E-mail: alaina.a.adderley@gmail.com

The BWER is a reflectivity signature related to updraft strength. This area of lower charge separation occurs because of the strong updraft limiting hydrometeor development (Ziegler et al. 2014; MacGorman et al. 2005; Chmielewski et al. 2020). Similarly to lightning jumps, lightning holes have been found to be indicative of the formation of a strong updraft in a Kansas supercell (MacGorman et al. 2005). The edges of this lightning hole have higher flash densities, which are sometimes referred to as the lightning ring (Payne et al. 2010). This pattern of lightning is not defined numerically and is instead a pattern identified subjectively. Much of the research on lightning holes has been for supercells (MacGorman et al. 2005; Payne et al. 2010; Stough et al. 2017; Kosiba et al. 2024;Ziegler et al. 2014); more research on other storm modes needs to be conducted.

This study looks at a storm from the Propagation, Evolution, and Rotation in Linear Storms (PERiLS) field campaign that exhibits these lightning patterns. One of the goals of this campaign was to understand the anatomy of a Quasi-linear convective system (QLCS) using a wide variety of instrumentation, including mobile radars, a variety of sondes, and a Lightning Mapping Array (LMA) network (Kosiba et al. 2024). Field campaigns such as this one provide a wealth of lightning data that can be used to analyze patterns and trends, narrowing the gap in the research.

Very little has been done to study the behavior of storms addressing lightning holes with lightning jumps and dives together, despite them being related to updraft intensity. Since lightning jumps/dives and lightning holes are all related to updraft strength, it may be hypothesized that there is a relationship between them. There were not many expectations going into this research on how these features would behave or in a QLCS; as there is no published evidence of lightning holes analyzed in this way or in this storm mode. Ultimately, a greater understanding of how lightning patterns relate to intensification in a wide variety of storm modes could aid in operational warning lead times and warning confidence.

2. Data and Methods

The PERiLS campaign collected data from QLCSs during 2022 and 2023 in the Southeastern US. Among the equipment used was the National Severe Storms Laboratory (NSSL) Mobile LMA (Chmielewski et al. 2022; Kosiba et al. 2024). Lightning can be measured in a multitude of ways; the gold standard for measuring total, 3D lightning flashes is the LMA. An LMA system is a network of sensors in close enough range of each other (10s of km) which record the Very High Frequency (VHF) lightning radiation signals generated by lightning channels, and then triangulated in time and space (Rison et al. 1999). These networks provide great lightning data but are limited in range and numbers, leading to mobile systems like the one used in PERiLS.

On March 22, 2022, a QLCS moved through Mississippi and Alabama. PERiLS Intensive Observation Periods (IOPs) were selected based on storm longevity and severity. This study analyzes an isolated supercell out ahead of the QLCS that merges with the system. [Fig. 1]

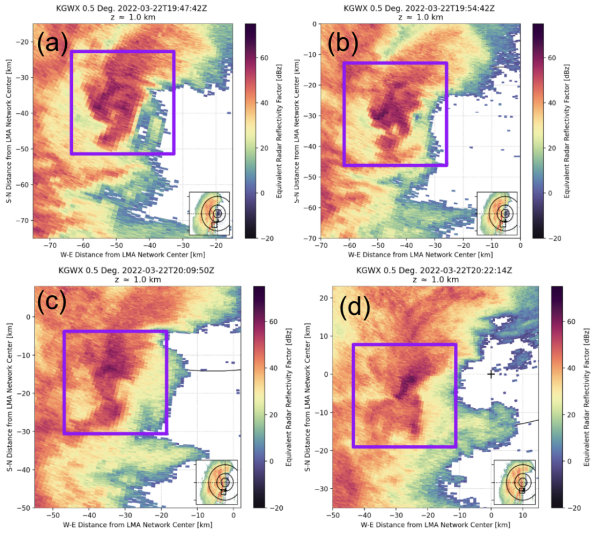

FIG. 1. Radar progression through the merge process at a 0.5 degree tilt. The subset map shows a zoomed out location, with the rings indicating distance from the KGWX radar. Each image is a 70km^2 frame approximately 150 km away from KGWX. (a) At 19:47 UTC cell is isolated out ahead of the QLCS; (b) Cell begins it's merge at 19:54 UTC; (c) Cell is mostly merged into the QLCS by 20:09 UTC; (d) Cell is fully merged into the QLCS by 20:22 UTC.

LMA data were sorted and grouped into flashes (Bruning 2015). Each source was required to have a maximum reduced chi-squared value of 1, and were grouped into flashes if they were within 3km of each other; and 0.15s intervals with a maximum flash duration of three seconds (Bruning 2015; Fuchs et al. 2016). In order for a flash to be included in this analysis, it needed to contain at least 10 VHF sources. Storm tracks for the duration of the cell were created using Tobac (Heikenfeld et al. 2019) and used the five-minute flash extent density, on a 1 km x 1 km grid. Each cell needed 4.5 flashes per minute at a minimum to be tracked, and the tracks were manually adjusted for short gaps in the flash rates. Any flash that initiated within 20 km of the storm track was considered a part of the storm. This track was compared to a manual track using the coordinates noted from the subjective lightning hole analysis, and was found to be a reasonable match.

Radar data were collected from the KGWX radar in Jackson, Mississippi. The radar data were plotted using Py-ART (Helmus et al. 2016), with the LMA data filtered

to within the radar angle of elevation +/- 2.5 km. One minute of lightning data were plotted after the start of the scan. Plots were then analyzed to determine the lightning hole location in regard to the BWER. Each instance of a lightning hole at a given altitude was noted.

The flash rates associated with the tracked cell were used to identify lightning jumps using a variation of the two standard deviations (2σ) algorithm. This algorithm defines a lightning jump as an increase of at least two standard deviations from the previous 10-minute flash rate changes and analyzes flash rates in two-minute intervals (Schultz et al. 2009). A jump is continued in time over the duration of increasing flash rates. A dive was treated as the negative of the jump algorithm.

An analysis of the cell was conducted to identify lightning holes within the IDL XLMA Lightning Mapping Array Display from New Mexico Tech. Lightning holes are a subjective pattern with many shapes that are not often a full circle. [Fig. 2]. The lightning holes were analyzed for each 1-km layer in the vertical in two-minute intervals, with timing, location, shape, and general behavior noted.

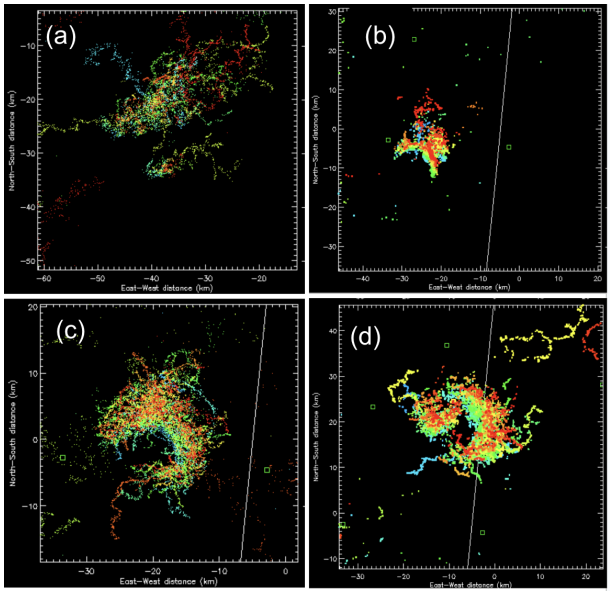

FIG. 2. LMA VHF sources indicating variations in lightning hole shapes exhibited during this cell. (a) Corridor at 19:59 UTC in the 0-20 km range. (b) Segment of a circle at 20:18 UTC in the 3-4 km range. (c) Cresent shaped lightning hole at 20:26 UTC in the 0-20 km range. (d) Nearly enclosed lightning hole at 20:42 UTC in the 9-10 km range.

The lightning hole analyses were then compared to these jumps/dives and overall flash rate trends by looking at each altitude in each two-minute interval, noting patterns such as the storm's progression in the merge, tornadogenesis timing, the flash rate trend, and the lightning holes' shape and behavior. Lightning holes can come in a wide variety of shapes and sizes; the two that are distinctly noted are corridor and hole. A corridor lightning hole resembles a channel of little to no lightning activity surrounded by two unconnected areas of lightning activity. The lightning holes are most commonly in the shape of a half circle or a C, but they can occur in any sized segment of a circle, including a fully closed one. [Fig. 2]

3. Results and Discussion

The cell of interest was isolated when it entered the range of the LMA network at 19:25 UTC. Initial tornadogenesis occurred at 19:35 UTC, and the tornado lasted just three minutes. The ending of this tornado coincided with the timing of the first lightning dive, which lasted roughly four minutes and reached flash rates of 100 flashes per minute (fpm) which was about 25 fpm lower than the prior 10 minutes [Fig. 4]. At this time, the lightning hole formed, its shape resembling a corridor at 7-9 km. At 19:44 UTC, a jump initiated and lasted five minutes. This increase in flash rates is the first of a pattern seen for many of the lightning hole expansions, where the expansion is followed by an increase in the flash rates. The lightning hole during this time expanded downward a kilometer; this new level formed as a hole rather than a corridor. [Fig. 3] The lightning jump ended with a peak of 167 fpm. Starting at 19:48 and persisting for 6 minutes, a decline in flash rates accompanied the mid levels of the lightning hole progressing into a hole.

At 19:54 UTC, the cell began its merge into the QLCS. This happened in conjunction with a slight increase in flash rates and an expansion of the lightning hole down a kilometer. At 19:56 UTC, the decrease in flash rates returned, paired with an increase in the height of the lightning hole by 1 km. This upward expansion took the form of a corridor. At 19:58 UTC, the cell entered a lightning dive state that lasted for approximately eight minutes. During this time, the lightning hole expanded vertically in both directions until it reached an extent of 3-11 km, where it would remain for most of the remaining time. The lightning hole in the middle levels of the cell started to form a strong signature.

At 20:06 UTC, the flash rates increased, and the lightning hole dissipates in the 4-5 km layer, beginning a pattern of sporadic hole dispersions. At 20:08 UTC, the cell was mostly merged into the QLCS and flash rates decreased. Two minutes later, those flash rates increased slightly, and the intermittent hole now spanned a 3 km range in the mid levels of the cell. From 20:12-20:14 UTC, there is the second-lowest flash rate value at just 30 fpm.

At 20:16 UTC, a variety of events occur. Missing radar scans span a timeframe of 4 minutes, and when radar returns, the cell is fully merged into the QLCS. During this gap in radar coverage, tornadogenesis also occurs, forming a tornado that would last roughly 18 minutes, ending at 20:35 UTC. Another feature occurring at 20:16 UTC was the initiation of the longest lightning jump that this

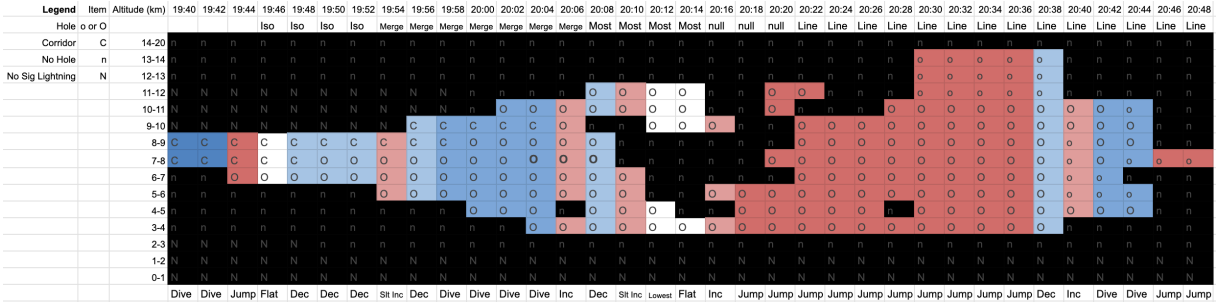

FIG. 3. Lightning hole over time with respect to height. Timing spans only the time where the lightning hole occurred. Black cells are where there is no lightning hole, and white are where the flash rates do not change. Blue cells indicate decreasing flash rates while red cells indicate increasing flash rates.

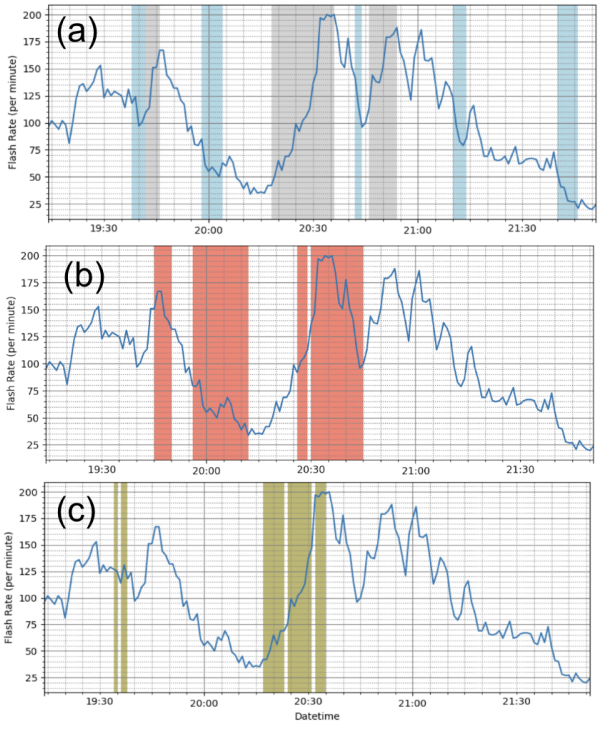

FIG. 4. Time series analyses of flashes per minute throughout the time the cell was in the LMA domain. The line is the flashes per minute. (a) Grey indicates lightning jumps, blue indicates lightning dives. (b) Red indicates times when there was a lighting hole. (c) Yellow indicated times there was a tornado.

cell experienced, lasting 20 minutes and eventually leading to peak flash rate values of 200 fpm and the lightning hole presenting up to 14 km. This change in both lightning patterns is likely related to the completed merge into the QLCS, as the cell now has more potentially charged cloud and precipitation particles to create discharges. This resulted in higher flash rates, and higher lightning hole elevation and possible dynamic changes. During this period of time, the lightning hole continues to dissipate and reform at various levels and times – until the peak flash rates ended with lightning hole presentation at all levels.

At 20:38 UTC, the flash rates begin to decrease. Two minutes later, flash rates increase temporarily as the hole contracts to 4-11 km. The increase in flash rate after vertical contraction is consistent with the increase in flash rates after vertical expansion. At 20:42 UTC, flashes decrease at a lightning dive rate for 4 minutes before another lightning jump is identified as the hole contracts down to just 7-8 km. This jump lasts just four minutes until 20:48, after which the hole dissipates and does not return.

The lightning jump persists until 20:54 UTC before the storm enters a gradual decline. It experiences two more lightning dives before it moves out of range of the LMA with final flash rates of 20 fpm.

4. Conclusion

This analysis of the relationship between lightning holes and lightning jumps/dives creates a comparison between these spatial and temporal analyses that had not previously been done. The results of this analysis are:

- Lightning holes exist not only in isolated supercells but also in QLCSs.
- The lightning hole in this study began in the mid-levels of the storm and expanded vertically from there. The storm exhibited similar behavior in flash rate patterns to the expansions in its end of life as it contracted.
- This cell exhibited an alternating flash rate pattern, where the duration of the vertical expansion/contraction occurred during a time of decreasing flash rates, but many of the times the altitude changes whose flash rates briefly increased.
- The merging of the supercell into the QLCS likely had an effect on the lightning hole behavior and the flash rate trends.

This case study provides insight into some of the potential behaviors of lightning holes and flash rate patterns in a mixed-mode storm. Future research involving more storms that start out isolated and then merge into a QLCS will help solidify these findings. Analyzing other storm modes and environments could provide a greater understanding of lightning behavior in general.

The missing radar data provided some additional limitations due to the timing of the events. More analyses on updraft proxies could prove insightful for this storm. Additionally, we do not know how these features varied before or after the storm was in the LMA domain. Understanding this relationship between lightning holes and lightning jumps/dives will ultimately aid in early warning lead times as well as forecaster confidence.

5. Acknowledgments

This research was supported by NSF grant AGS 2050267 as a part of the National Weather Center Research Experience for Undergraduates (NWC REU). This program was made possible by Daphne Ladue and Alex Marmo. A special thank you also goes out to Alyssa Bates for her assistance and coaching while writing this paper.

References

Bruning, 2015: lmatools: lmatools-v0.5z-stable. Zenodo, URL https://doi.org/10.5281/zenodo.32510, doi:10.5281/zenodo.32510.

Chmielewski, V., 2022: https://doi.org/10.26023/R0K6-AXR5-YZ00. PERiLS_2022: NSSL deployable lightning mapping array data. doi:https://doi.org/10.26023/R0K6-AXR5-YZ00.

Chmielewski, V. C., D. R. MacGorman, C. L. Ziegler, E. DiGangi, D. Betten, and M. Biggerstaff, 2020: Microphysical and transportive contributions to normal and anomalous polarity subregions in the 29–30 may 2012 kingfisher storm. **125 (16)**, e2020JD032 384, doi:10.1029/2020JD032384, URL https://agupubs.onlinelibrary.wiley.com/doi/10.1029/2020JD032384.

Darden, C. B., D. J. Nadler, B. C. Carcione, R. J. Blakeslee, G. T. Stano, and D. E. Buechler, 2010: Utilizing total lightning information to diagnose convective trends. **91 (2)**, 167–176, doi:10.1175/2009BAMS2808.1, URL https://journals.ametsoc.org/doi/10.1175/2009BAMS2808.1.

Fuchs, B. R., E. C. Bruning, S. A. Rutledge, L. D. Carey, P. R. Krehbiel, and W. Rison, 2016: Climatological analyses of LMA data with an open-source lightning flash-clustering algorithm. **121 (14)**, 8625–8648, doi:10.1002/2015JD024663, URL https://agupubs.onlinelibrary.wiley.com/doi/10.1002/2015JD024663.

Goodman, S. J., and Coauthors, 2013: The GOES-r geostationary lightning mapper (GLM). **125-126**, 34–49, doi:10.1016/j.atmosres.2013.01.006, URL https://linkinghub.elsevier.com/retrieve/pii/S0169809513000434.

Heikenfeld, M., P. J. Marinescu, M. Christensen, D. Watson-Parris, F. Senf, S. C. Van Den Heever, and P. Stier, 2019: tobac 1.2: towards a flexible framework for tracking and analysis of clouds in diverse datasets. **12 (11)**, 4551–4570, doi:10.5194/gmd-12-4551-2019, URL https://gmd.copernicus.org/articles/12/4551/2019/.

Helmus, J. J., and S. M. Collis, 2016: The python ARM radar toolkit (py-ART), a library for working with weather radar data in the python programming language. doi:10.5334/jors.119.

Kosiba, K. A., and Coauthors, 2024: The propagation, evolution, and rotation in linear storms (PERiLS) project. **105 (10)**, E1768–E1799, doi:10.1175/BAMS-D-22-0064.1, URL https://journals.ametsoc.org/view/journals/bams/105/10/BAMS-D-22-0064.1.xml.

MacGorman, D. R., W. D. Rust, P. Krehbiel, W. Rison, E. Bruning, and K. Wiens, 2005: The electrical structure of two supercell storms during STEPS. **133 (9)**, 2583–2607, doi:10.1175/MWR2994.1, URL http://journals.ametsoc.org/doi/10.1175/MWR2994.1.

Payne, C. D., T. J. Schuur, D. R. MacGorman, M. I. Biggerstaff, K. M. Kuhlman, and W. D. Rust, 2010: Polarimetric and electrical characteristics of a lightning ring in a supercell storm. doi:10.1175/2009MWR3210.1, URL https://journals.ametsoc.org/view/journals/mwre/138/6/2009mwr3210.1.xml.

Rison, W., R. J. Thomas, P. R. Krehbiel, T. Hamlin, and J. Harlin, 1999: A GPS-based three-dimensional lightning mapping system: Initial observations in central new mexico. **26 (23)**, 3573–3576, doi:10.1029/1999GL010856, URL https://agupubs.onlinelibrary.wiley.com/doi/10.1029/1999GL010856.

Schultz, C. J., W. A. Petersen, and L. D. Carey, 2009: Preliminary development and evaluation of lightning jump algorithms for the real-time detection of severe weather. **48 (12)**, 2543–2563, doi:10.1175/2009JAMC2237.1, URL http://journals.ametsoc.org/doi/10.1175/2009JAMC2237.1.

Steiger, S. M., R. E. Orville, and L. D. Carey, 2007: Total lightning signatures of thunderstorm intensity over north texas. part i: Supercells. doi:10.1175/MWR3472.1, URL https://journals.ametsoc.org/view/journals/mwre/135/10/mwr3472.1.xml.

Stough, S. M., L. D. Carey, C. J. Schultz, and P. M. Bitzer, 2017: Investigating the relationship between lightning and mesocyclonic rotation in supercell thunderstorms. **32 (6)**, 2237–2259, doi:10.1175/WAF-D-17-0025.1, URL https://journals.ametsoc.org/doi/10.1175/WAF-D-17-0025.1.

Takahashi, T., 1984: Thunderstorm electrification—a numerical study. **41 (17)**, 2541 – 2558, doi:10.1175/1520-0469(1984)041⟨2541:TENS⟩2.0.CO;2, URL https://journals.ametsoc.org/view/journals/atsc/41/17/1520-0469_1984_041_2541_tens_2_0_co_2.xml, place: Boston MA, USA Publisher: American Meteorological Society.

Vacek, A. D., L. D. Carey, and S. M. Stough, 2017: 2.4a kinematic, microphysical and lightning properties of a tornadic and nontornadic supercell during VORTEX-SE.

Williams, E., and Coauthors, 1999: The behavior of total lightning activity in severe florida thunderstorms. **51 (3)**, 245–265, doi:10.1016/S0169-8095(99)00011-3, URL https://linkinghub.elsevier.com/retrieve/pii/S0169809599000113.

Ziegler, C. L., E. R. Mansell, K. M. Calhoun, and D. R. MacGorman, 2014: Impact of kinematics, microphysics, and electrification on the formation of lightning-weak holes in a simulated supercell storm.